COOPERATIVITY IN THE PHOTOCYCLE OF PURPLE MEMBRANE OF *HALOBACTERIUM HALOBIUM* WITH A MECHANISM OF FREE ENERGY TRANSDUCTION

Rafi KORENSTEIN, Benno HESS and Mario MARKUS
Max-Planck-Institut für Ernährungsphysiologie, Rheinlanddamm 201, 4600 Dortmund, FRG

Received 12 March 1979

1. Introduction

The purple membrane of *Halobacterium halobium* contains a single protein to which a retinal is bound via a protonated Schiff base [1,2]. The structure and the organization of this retinal–protein complex, bacteriorhodopsin (BR), within the purple membrane was investigated by X-ray diffraction and electron microscopy [3–7]. These studies showed that bacteriorhodopsin is a globular protein composed of seven closely packed α-helical segments which extend roughly perpendicular to the plane of the membrane, spanning a 48 Å bilayer. Bacteriorhodopsin molecules are arranged in a two dimensional array, forming an almost perfect crystal lattice of space group P_3. Thus, three protein molecules are in direct contact, forming a trimeric cluster with the retinal chromophore orientated at $\leqslant 27^\circ$ with the plane of the membrane [8].

Such an organization of the molecules imposes strong protein–protein interactions, which might result from the large contact areas between helical domains. Furthermore, the chemical sequence [9] suggests additional interactions through terminal peptide chains as well as amino acid residues. A consequence of these interactions is the complete immobilization of the protein within the purple membrane, allowing no rotational freedom to bacteriorhodopsin even in the minute time range [8]. Moreover, an electronic coupling between the retinal chromophores is shown by the circular dichroic spectrum (CD) of the purple membrane. The visible circular dichroism of purple membrane consists of intense positive and negative bands with a crossover at the wavelength of the absorption maximum [10,11]. This CD spectrum was shown [10,12,13] to arise from two contributions: a positive band due to a retinal bound to the protein and positive and negative bands (bilobe) due to the exciton interaction between chromophores of neighbouring proteins. Thus, at such a high level of protein organization one would also expect to observe a kinetic coupling among the three bacteriorhodopsin molecules which constitute the trimeric cluster.

This study shows the existence of such a kinetic coupling by demonstrating the dependence of the photocycle kinetics of a bacteriorhodopsin molecule on the conformational state of its nearest neighbours. The results fit a cooperative mechanism of free energy transduction based on subunit–subunit interactions within a trimer.

2. Materials and methods

Purple membrane was isolated [1], suspended and irradiated under light-adapted conditions (all-*trans*) with a 400 W W–I_2 lamp by light > 500 nm in the experimental set given in [14]. The light intensity was varied by means of neutral filters, so that different steady state concentrations of M^{412} were obtained. The measuring light was lead and detected as given in [14]. The temperature was measured by a Cu-Constantan thermocouple connected to a Fluke 2100 A digital thermometer (± 0.1°C). The thermocouple was inserted into the sample solution at the illuminated area, in order to detect possible local heat during the

Table 1
Decay kinetics[a] from different photostationary levels of M^{412} at −20°C

No	$[BR]_0$[c] (μM)	$[M^{412}]$[d] (μM)	$[M^{412}]/[BR]_0$	k_a (s^{-1})	k_b (s^{-1})
1	20	11 8	59%	3 66 ± 12 (0 21 ± 01)[b]	0 35 ± 01 (0 78 ± 01)[b]
2		7 0	35%	2 33 ± 26 (0 11 ± 01)	0 33 ± 01 (0 88 ± 01)
3		3 6	18%	1 18 ± 17 (0 15 ± 03)	0 32 ± 01 (0 84 ± 03)
4		1 8	9%	1 07 ± 09 (0 21 ± 02)	0 31 ± 01 (0 84 ± 03)
5	5	3 0	60%	3 49 ± 44 (0 17 ± 02)	0 42 ± 01 (0 83 ± 01)
6	20	3 0	15%	1 21 ± 22 (0.18 ± 04)	0 39 ± 01 (0 81 ± 04)
7	30	3 0	10%	1 05 ± 27 (0 29 ± 13)	0 36 ± 05 (0 70 ± 13)

[a] Purple membrane (BR^{570}) was suspended in ethylene glycol–water 1 1 mixture, 50 mM phosphate buffer (pH 7 2)
[b] Amplitudes are shown in parentheses
[c] Using extinction coefficient of 63 000 (M^{-1}, cm^{-1})
[d] Using a ratio of 0 5 between the difference extinction coefficient of M^{412} (at 412 nm) and the extinction coefficient of BR^{570}

photobleaching experiments The light flux was measured with a Tektronix J16 digital photometer Optimizations were performed by a least square program from the Harwell Subroutine Library (VCO5A for the sum of exponentials and VAO5A for the cooperativity model)

3 Results and discussion

The measured decay of M^{412} from the different photostationary levels back to the equilibrium state ($BR^{570}_{all\text{-}trans}$) could be fitted by a sum of two exponentials yielding the decay rate constants (k_a and k_b) shown in table 1 The total concentration of bacteriorhodopsin is denoted by $[BR]_0$ We see that the rates are strongly correlated with the degree of occupancy of M^{412}, namely the $[M^{412}]/[BR]_0$ ratio It should be stressed that no significant changes in the formation rates of M^{412} were observed In order to eliminate the possibility that the observed kinetics are due to specific solute–purple membrane interactions, we also performed the kinetic measurements in the absence of ethylene glycol in the presence of basal salt and observed a similar correlation between the decay rates and the occupancy of M^{412} (table 2)

The observation that M^{412} decays as a sum of two exponentials is explained by the existence of two conformers of M^{412} which we have called M and M′ [14] These decays can be considered here as pseudo-first order reactions in spite of the protonation step involved, since the pH is kept constant due to buffering The trimeric structural organization of bacteriorhodopsin together with the observed correlation between the overall decay rates and the degree of occupancy of M^{412} suggests that the corresponding intrinsic decay rates depend on the conformational state of the nearest neighbouring molecules

Since the bilobe in the CD spectrum of purple membrane arises from exciton interactions between

Table 2
Decay kinetics[a] from different photostationary levels of M^{412} at −16°C

$[BR]_0$[c] (μM)	$[M^{412}]$[d] (μM)	$[M^{412}]/[BR]_0$	k_a (s^{-1})	k_b (s^{-1})
20	9 0	45%	2 78 ± 62 (0 25 ± 04)[b]	1 08 ± 01 (0 75 ± .05)[b]
	1 9	9 5%	1 54 ± 03 (0 61 ± 07)	0 64 ± 08 (0 39 ± 07)
5	2 45	49%	2 59 ± 28 (0 32 ± 06)	0 95 ± 06 (0 68 ± .06)
30	2 55	8 5%	1 06 ± 03 (0 63 ± 04)	0 42 ± 03 (0 37 ± 05)

[a] Purple membrane was suspended in aqueous solution of basal salts, 50 mM phosphate (pH 6 0)
[b,c,d] See legend to table 1

Table 3
Decay kinetics[a] from different photostationary levels of M^{412} at +20°C

$[BR]_o$[c] (μM)	$[M^{412}]$[d] (μM)	$[M^{412}]/[BR]_o$	k_a (s^{-1})	k_b (s^{-1})
	7.8	58%	0.093 ± .010 (0.37 ± .05)[b]	0.027 ± .003 (0.62 ± .06)[b]
13.5	3.8	28%	0.087 ± .023 (0.27 ± .13)	0.027 ± .005 (0.73 ± .13)
	1.9	14%	0.118 ± .026 (0.13 ± .03)	0.027 ± .002 (0.87 ± .03)
3.4	2.7	80%	0.128 ± .011 (0.37 ± .04)	0.034 ± .002 (0.63 ± .04)
20.2	2.8	14%	0.105 ± .033 (0.21 ± .14)	0.032 ± .004 (0.78 ± .12)

[a] Purple membrane was suspended in aqueous solution of basal salts, 50 mM phosphate buffer (pH 6.0) and saturated with diethyl-ether
[b,c,d] See legend to table 1

the chromophores of protein molecules within a trimer, its existence can serve as a measure of the degree of electronic coupling between adjacent chromophores. The exciton interaction can be decoupled by suspending the purple membrane in basal salts and then saturating the solution with diethylether [15]. In addition, the presence of ether induces rotation of the bacteriorhodopsin molecules within the membrane [16]. Therefore, we have chosen to study the photocycle under conditions where exciton coupling between the chromophores is abolished in order to find out whether a correlation between kinetic and spectroscopic coupling exists. The experiments, done in the same way as for the fully coupled system, are given in table 3. It is seen that the decay rates do not change essentially with the increase of M^{412} occupancy.

The findings suggest that the disappearance of exciton coupling between the chromophores is correlated with the disappearance of the kinetic coupling between the proteins. However, an analysis of the kinetics in the presence of guanidine–HCl indicates that exciton coupling is not an obligatory condition for kinetic coupling. In fact, no correlation between the rate constants and the degree of occupancy is seen in the presence of guanidine–HCl (table 4), although the latter one does not effect the excitonic band in the CD spectra of BR [17]. In addition, we have analyzed the possibility of rotational mobility of bacteriorhodopsin molecules in the presence of guanidine–HCl by analyzing the time dependence of the anisotropy factor in the thermal decay of the BR^{LA} state produced by photoselection analogous to the method described in [8]. We found that the anisotropy factor does not change over a minute time range indicating that the rotational immobility is not affected by guanidine–HCl (R. K., B. H., unpublished results). We therefore suggest that guanidine–HCl may interfere with the protein–protein interphase in the trimeric unit without affecting the relative orientation of the chromophores.

Table 4
Decay kinetics[a] from different photostationary levels of M^{412} at +20°C

$[BR]_o$[c] (μM)	$[M^{412}]$[d] (μM)	$[M^{412}]/[BR]_o$	k_a (s^{-1})	k_b (s^{-1})
	13.8	69%	0.28 ± .04 (.47 ± .16)[b]	0.11 ± .02 (.53 ± .16)[b]
	9.8	49%	0.30 ± .01 (.47 ± .10)	0.12 ± .01 (.53 ± .11)
	5.0	25%	0.24 ± .01 (.60 ± .07)	0.10 ± .01 (.40 ± .06)
20	4.0	20%	0.25 ± .05 (.60 ± .20)	0.09 ± .02 (.40 ± .20)
	2.0	10%	0.23 ± .01 (.63 ± .09)	0.09 ± .01 (.37 ± .09)
	1.0	5%	0.32 ± .06 (.48 ± .15)	0.11 ± .03 (.52 ± .16)

[a] Purple membrane (20 μM) was suspended in aqueous solution containing 8 M guanidine–HCl, 0.05 M glycine (pH 8.0)
[b,c] See legend to table 1
[d] Using a ratio of 0.75 between the difference extinction coefficient of M^{412} (at 412 nm) and the extinction coefficient of BR^{570}

4 Cooperative mechanism of free energy transduction

The construction of the cooperativity model for the photocycle kinetics is based on the following considerations

(i) Bacteriorhodopsin can be found in two interconvertible forms undergoing separate photocycles [1,18] Under our experimental conditions we investigate the photocycle of $BR^{570}_{all\text{-}trans}$ which consists of several intermediates as shown by the scheme in fig 1 This scheme extends earlier schemes [19–22] including L'' (a photochemical product of L) [23] and two conformations of L^{550} and M^{412} (denoted by L, L' and M, M', respectively) described in [14]

(ii) By inserting the kinetic constants from [14,19] into the differential equations of the photocycle, it can be shown that, under our experimental conditions, the short circuit L, L' → L'' → BR can be neglected It can further be shown that we can neglect the reaction K → BR and that we can consider K, L and L' to be in a quasi-stationary state As a result, the system described in fig 1 reduces to a cycle where only the BR, M and M' states are to be considered M and M' equilibrate with h_1 and h_2

(iii) Since, under the experimental conditions described, the conversion yield of BR^{570} into M^{412} was ⩽ 66%, the model is limited only to those states where at most two molecules of the trimer adopt the M^{412} conformations Indeed, the probability that all three molecules of the trimer are in the M^{412} state is too small under these conditions

(iv) No photochemical reactions of M^{412} [24] were considered because BR was excited with light > 500 nm Furthermore, the O^{660} intermediate was neglected in the photocycle scheme since it was not formed under our experimental conditions

(v) It is assumed that the interaction among bacteriorhodopsin molecules occurs only within a trimeric cluster, whereas any interaction between clusters is neglected

(vi) The intrinsic formation rates k_2 and k_2' in fig 1) are assumed to be independent of the neighbouring molecules in the cluster, because we found no significant changes in the overall formation rates in the various experiments

The model resulting from assumptions (i) to (vi) is illustrated in the upper three rows of fig 2 The dependence of the intrinsic decay rates of M and M' on the conformational state of the neighbouring molecules is described by the introduction of four rates, k^0_{D1}, k^1_{D1}, k^0_{D2} and k^1_{D2}, instead of k_{D1} and k_{D2} (fig 1) k^0_{D1} and k^0_{D2} refer to the decay when no other molecule in the trimer is in the M or M' state

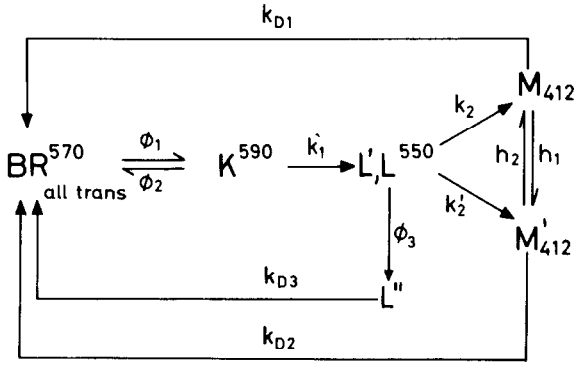

Fig 1 Schematic diagram of the photocycle of bacteriorhodopsin Φ_1 and Φ_2 are the quantum yields

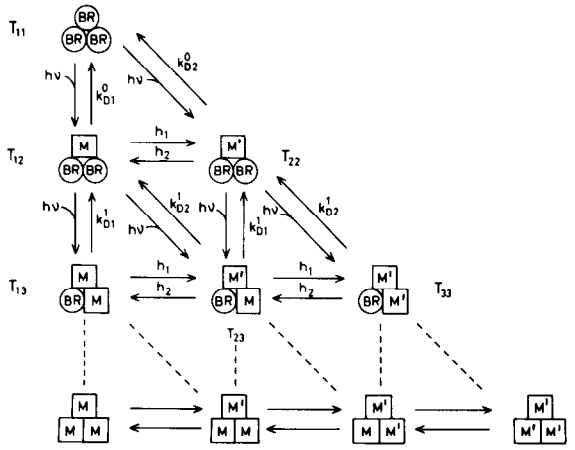

Fig 2 Cooperativity model of the photocycle Transitions between trimeric states in purple membrane assuming a two state cycle The broken lines indicate transitions to states which are neglected since the total conversion of BR into M was ⩽ 66% in the experiments

The equations describing the time dependence of the concentrations of the trimeric states as a function of the total light power input per unit surface (E_T) are given by:

$$\frac{dT_{ij}}{dt} = -(j-i)\,h_1\,T_{ij} + (j-i+1)\,h_1\,T_{i-1,j}\,\bar{\delta}_{i1} + ih_2\,T_{i+1,j}\,\bar{\delta}_{ij} - (i-1)\,h_2\,T_{ij} + K_1 f_{5-j}\,T_{i,j-1}\,\bar{\delta}_{ij} - f_{4-j}\,T_{ij}\,\bar{\delta}_{3j} + K_2 f_{5-j}\,T_{i-1,j-1}\,\bar{\delta}_{i1} + (j-i+1)\,k_{D1}^{j-1}\,T_{ij+1}\,\bar{\delta}_{3j} - (j-i)\,k_{D1}^{j-2}\,T_{ij} + ik_{D2}^{j-1}\,T_{i+1,j+1}\,\bar{\delta}_{3j} - (i-1)\,k_{D2}^{j-2}\,T_{ij} \quad (1)$$

$$i = 2,3 \quad j = 2,3 \quad i \leqslant j$$

$$T_{11} = [BR]_0/3 - T_{12} - T_{22} - T_{13} - T_{23} - T_{33}$$

$\bar{\delta}_{ij}$ has the complementary meaning of the Kronecker symbol, i.e., $\bar{\delta}_{ij} = 1$ for $i \neq j$ and $\bar{\delta}_{ij} = 0$ for $i = j$. The functions f are given by:

$$f_n(X) = \frac{q \cdot \Phi_1 E_T}{hcd \int_0^\infty \frac{1}{\lambda} tr(\lambda)d\lambda} \int_0^\infty \left(1 - 10^{-nd\epsilon_{BR}(\lambda)X}\right) tr(\lambda)d\lambda$$

The K values are defined by $K_1 = 1/(1 + k_2'/k_2)$ and $K_2 = 1 - K_1$.

In these equations we have considered that the sample was irradiated through a broad filter with spectral characteristics described by the transmission function $tr(\lambda)$, so that $dI/d\lambda$ is proportional to $tr(\lambda)$ (I is the light transmitted). h is Planck's constant, c is the velocity of light and d is the thickness. n is the possible number of molecules in a trimer to undergo a given transition. The factor q accounts for the effective light flux.

5. Simulation and fitting of the cycle kinetics

The experimentally determined quantity to be fitted by the model is the absorbance at 412 nm given by:

$$A = \Delta\epsilon_{412}(T_{12} + T_{22} + 2\,(T_{13} + T_{23} + T_{33})) \quad (2)$$

where $\Delta\epsilon_{412} = 31\,000\ M^{-1}\ cm^{-1}$. The differential equations for the T_{ij} were integrated using a program developed by Gear [25]. The resulting functions of time were inserted in eq. (2) to obtain A, which was fitted to the decay kinetics given in table 1 and the measurements of the photostationary state given in fig.3 simultaneously, optimizing the eight unknown parameters h_1, h_2, k_{D1}^0, k_{D2}^0, k_{D1}^1, k_{D2}^1, k_2'/k_2 and $q \cdot \Phi_1$. Since the error of measurement was approximately independent of the magnitude of the measurement, we fitted with equal weighting of all residuals. The total number of fitted measurement points was 247.

The characteristic times of the equilibration process between M and M′ are expected to be of the order of several seconds [14], so that the question arises, whether this process can be neglected in the calculations. We therefore performed the optimization with and without considering the equilibration and obtained no significant difference in the minimal

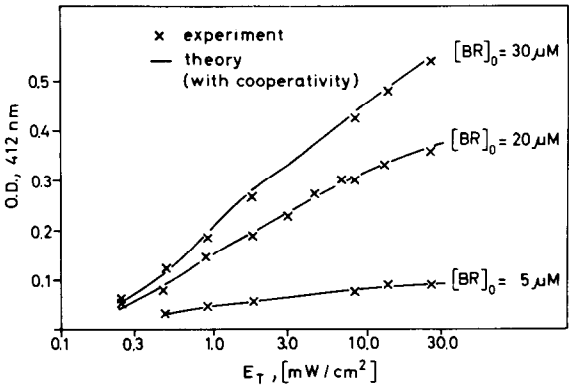

Fig.3. Dependence of the photostationary absorbance of M_{412} on the total light power input per unit surface for three different concentrations of bacteriorhodopsin. The experimental conditions are those given in table 1. The crosses are the experimental values. The curves correspond to the theory assuming cooperativity.

sum of squares (variance ratio = 1 09) so that the system can be described by a simplified model in which $h_1 = h_2 = 0$ The parameters which remain to be optimized are $k^0_{D1}, k^1_{D1}, k^0_{D2}, k^1_{D2}, q \quad \Phi_1$ and k'_2/k'_2 After performing the fitting, we found that it was only possible to determine the product of the parameters k'_2/k_2 and k^1_{D1}, i e , the expression $p = k'_2 \quad k^1_{D1}/k_2$ We obtained

$p \quad = 1\ 6 \pm 0\ 4\ s^{-1}$
$k^0_{D1} \quad = 0\ 27 \pm 0\ 03\ s^{-1}$
$k^0_{D2} \quad = 0\ 50 \pm 0\ 10\ s^{-1}$
$k^1_{D2} \quad = 3\ 5\ s^{-1}$
$q \quad \Phi_1 \quad = 0\ 867$

The standard deviation of the residuals of the fitted absorbance was 0 004 This is to be compared with the average measured absorbance of 0 1 We also performed the fitting by setting $k'_2 = 0$, which means that M′ can only be produced by an equilibration process of M and not as a product of L This yielded a variance of residuals 9 8-times higher than in the case without this constraint, so that we have to assume the existence of a branching mechanism In addition, it must be stressed that when assuming $k'_2 = 0$, we obtained $h_1 + h_2 = 2\ 5$, while there is experimental evidence [14] that this sum is $< 0\ 34$

Furthermore, we fitted the experiments by imposing $k^0_{D1} = k^1_{D1}$ and $k^0_{D2} = k^1_{D2}$, which would hold if there is no cooperativity The variance of the differences between theoretical and experimental values obtained in this case was 8-times higher than in the case where cooperativity was considered Furthermore we saw a predominance of systematic errors in case of the non-cooperativity model, while the errors in case of the cooperativity model were randomly distributed In view of these results, the cooperativity model strongly favours the suggested interpretation of our results

6. Conclusions

Direct evidence for interactions between the bacteriorhodopsin molecules in its native crystalline array is based on structural as well as functional properties of the purple membrane system Our findings support the notion of cooperativity in the decay kinetics of the 412 nm intermediates of the photocycle Here, protein–protein interactions effect the conformational states represented by the states M and M′ of the cycle Indeed, the correlation of all these properties under quasi-physiological conditions (although in open membrane sheets) is of greatest significance Furthermore, the application of experimental conditions reflecting differentially three properties of the system, sheds some light on the mechanism of kinetic cooperativity Whereas in the presence of basal salt or ethylene glycol rotational immobility, kinetic cooperativity as well as exciton coupling is observed, guanidine–HCl uncouples the cooperativity phenomenon, but does not lead to mobility or electronic decoupling, and ether affects all three functions These results suggest that in case of guanidine–HCl, although physical interaction in terms of electronic coupling might well be maintained, protein–protein interactions are strongly modified allowing kinetic cooperativity not to occur any more Obviously, guanidine–HCl affects the contact domains between bacteriorhodopsin molecules in a trimeric unit, a concept which is being further investigated in this laboratory

The observation of cooperativity in the purple membrane might be of importance for membrane functions in general (see [26,27]) It physiological significance is understood in terms of the overall efficiency of coupled molecular functions in the oligomeric forms of the membrane organization We visualize here cooperativity involved in transport and electrochemical gradient formation In case of the purple membrane, all these considerations should apply Here, the cooperativity displayed by the increase of the rate constants with increasing occupancy of the M or M′ state has a positive sign analogous to general autocatalysis allowing the amplification of dynamic states upon suitable cooperative coupling This positive cooperativity is relevant with respect to the relationship between the proton dissociation–association functions coupled to the photocycle in the purple membrane Recently, a high ratio of dissociated protons per M^{412} state in the range up to three at low light intensities and the decrease of this ratio to ~1 at saturating light intensities was found [28] This suggests an interaction between one molecule in the M^{412} state with its neighbouring molecules still in the

BR-state inducing proton transfer reactions in the latter molecules. Furthermore, it is significant that as a function of the light intensities the ratio of proton released per M^{412} state indicates negative cooperativity [28]. Here, we visualize that the positive cooperativity of the photocycle kinetics in connection with the negative cooperativity of the coupled proton transfer- and release-reactions are of significance for the stabilization of the overall process of vectorial proton transfer in the purple membrane of salt bacteria.

Acknowledgements

We thank Dr Th. Plesser for many valuable discussions, R. Müller for technical help and K. H. Dreher and K. H. Müller for programming assistance.

References

[1] Oesterhelt, D., Muntzen, M. and Schumann, L. (1973) Eur. J. Biochem. 40, 453–463.
[2] Lewis, A., Spoonhower, J., Bogomolni, R. A., Lozier, R. H. and Stoeckenius, W. (1971) Proc. Natl. Sci. USA 71, 4462–4466.
[3] Blaurock, A. E. and Stoeckenius, W. (1971) Nature New Biol. 233, 152–154.
[4] Blaurock, A. E. (1975) J. Mol. Biol. 93, 139–158.
[5] Henderson, R. (1975) J. Mol. Biol. 93, 123–138.
[6] Unwin, P. N. T. and Henderson, R. (1975) J. Mol. Biol. 425–440.
[7] Henderson, R. and Unwin, P. N. T. (1975) Nature 257, 28–32.
[8] Korenstein, R. and Hess, B. (1978) FEBS Lett. 89, 15–20.
[9] Ovchinnikov, Y. A., Abdulaev, N. G., Feigina, M. Yu, Kiselev, A. V. and Lobanov, N. A. (1977) FEBS Lett. 84, 1–4.
[10] Heyn, M., Bauer, P. and Dencher, N. (1975) Biochem. Biophys. Res. Commun. 67, 879–903.
[11] Becher, B. and Cassin, J. (1975) Biophys. J. 15, 66a.
[12] Bauer, P. J., Dencher, N. and Hey, M. (1976) Biophys. Struct. Mech. 2, 79–92.
[13] Becher, B. and Ebrey, T. (1976) Biochem. Biophys. Res. Commun. 69, 1–6.
[14] Korenstein, R., Hess, B. and Kuschmitz, D. (1978) FEBS Lett. 93, 266–270.
[15] Reed, T. and Hess, B. (1976) 67th Meet. Am. Soc. Biol. Chem. San Francisco, Abstr. 45.
[16] Heyn, M. P., Bauer, P. J. and Dencher, N. A. (1977) in: Biochemistry Membrane Transport (Semenza, G. and Carafoli, E. eds) FEBS Symp. no. 42, pp. 96–104, Springer Verlag, Berlin, Heidelberg.
[17] Yoshida, M., Ohno, K., Takenchi, Y. and Kagawa, Y. (1976) Biochem. Biophys. Res. Commun. 75, 1111–1116.
[18] Sperling, W., Carl, P., Rafferty, Ch. N. and Dencher, N. A. (1977) Biophys. Struc. Mech. 3, 79–94.
[19] Kung, M. C., Devault, D., Hess, B. and Oesterhelt, D. (1975) Biophys. J. 15, 907–911.
[20] Lozier, H., Bogomolni, R. A. and Stoeckenius, W. (1975) Biophys. J. 15, 955–962.
[21] Goldschmidt, C. R., Ottolenghi, M. and Korenstein, R. (1976) Biophys. J. 16, 839–943.
[22] Oesterhelt, D. and Hess, B. (1973) Eur. J. Biochem. 37, 316–326.
[23] Hurley, J. B., Becher, B. and Ebry, T. G. (1978) Nature 272, 87–88.
[24] Hess, B. and Kuschmitz, D. (1977) FEBS Lett. 74, 20–24.
[25] Gear, C. W. (1971) Numerical Initial Value Problems in Ordinary Differential Equations, Prentice Hall, Englewood Cliffs, NJ.
[26] Changeux, J. P. and Thiéry, J. (1968) in: Regulatory Functions of Biological Membranes (Järnefelt, J. ed) Biochim. Biophys. Acta Libr. 11, 116–138.
[27] Emrich, H. M. and Reich, R. (1974) Z. Naturforsch. 29c, 577–591.